

# FROM Modelling and Zircaloy-4 Oxidation Properties for CANDU fuel

By

A.G. McLean\*, F.C. Iglesias\*, C. Westbye\*

\*Ontario Power Generation, Inc., Toronto, Ontario, Canada

\*Bruce Power Inc., Tiverton, Ontario, Canada

## Abstract

As one of the principal barriers against the release of fission products into the primary heat transport system during a postulated accidents, definitive values for Zircaloy-4 properties and confidence its modelled behaviour is key to accident assessment. Recommended values and limits based on review of pertinent experimental data are presented for Zircaloy oxidation heat of reaction and Zircaloy-4 melting temperature. In addition, the validation of the Full Range Oxidation Model (FROM) code as well as statistical results and a comparison between FROM-3.0 and FROM-SFD are presented.

## 1 Introduction

A main goal of the study of nuclear fuel element performance and fission product under accident conditions is to be able to predict the activity release to containment for postulated accidents. The sheathing of nuclear fuel elements in a water-cooled reactor is one of the principal barriers against the release of fission products to containment. Accurate modelling of the different phenomena that influence the integrity of the sheathing is necessary.

The most common sheathing material is Zircaloy-4. This material was selected, from its physical and mechanical properties, its good corrosion resistance in water at operating temperatures. However, at the temperature levels reached during a postulated accident, the reaction between Zircaloy and steam can be very fast and can endanger sheath integrity. Also, the temperature increases may be large due to the quantity of heat (heat of reaction) liberated during the Zircaloy/steam oxidation process. In case of very high calculated temperature escalation, the melting of the Zircaloy sheath may challenge the integrity of the pressure tube.

To model the oxidation process, parabolic rate kinetics correlations may be used to estimate oxide layer thickness for thin oxide layers during simple ramp-and-hold temperature transients. For complex temperature transients (fast sequence of heating and cooling, thick oxide layers and oxygen starvation), diffusion based calculation should be used to that predict the resulting oxygen profile accurately enough for subsequent calculation of sheath deformation.

The Canadian Nuclear Industry has developed two codes for this purpose. The first code, FROM 3 (Full Range Oxidation Model) simulates the Zircaloy-4/steam reaction and oxygen redistribution during an arbitrary temperature transient. The second, FROM.SFD (FROM. Severe Fuel Damage) models both, the Zircaloy-4/steam reaction and the Zircaloy-4/UO<sub>2</sub> interaction.

This paper presents in Section 2, recommend values for the heat of reaction and the Zircaloy-4 (as-received) solidus temperature (melting temperature). In section 3, the validation of FROM 3 and a statistical assessment of this validation and, in section 4, a comparison between FROM 3 and FROM.SFD for the common are of their range of applicability.

## 2 Zircaloy-4 Properties

Two properties are important for the assessment of Zircaloy heat-up during oxidative phases of postulated accident scenarios: the heat of reaction and the Zircaloy-4 melting temperature. The following stoichiometric equation describe the reaction between Zircaloy-4 and steam:



This generated heat (heat of reaction) and the heat produced by the decay of fission product are the mayor contributors to reactor heat-up during postulated accidents. If the sheath temperature increase reaches the

Zircaloy melting temperature, the molten material may dissolve the  $\text{UO}_2$  liberation of fission products and/or challenge the integrity of the pressure tubes.

## 2.1 Heat of Reaction

The heat of reaction can be calculated using thermochemical enthalpy data. Commonly available thermochemical data for  $\text{ZrO}_2(\text{s})$  and  $\text{H}_2\text{O}(\text{g})$  has been reviewed. Barin<sup>1</sup> reports  $\text{ZrO}_2(\text{s})$  data ranging from 298K to 2900K, Cordfunke's<sup>2</sup> reports data for both  $\text{ZrO}_2(\text{s})$  and  $\text{H}_2\text{O}(\text{g})$  between 298K and 2900K and the CRC Handbook of Chemistry<sup>3</sup> between 298 and 2000 K.

Figure 1 compares the heat of reaction reported by Barin and Cordfunke for the  $\text{ZrO}_2(\text{s}) / \text{H}_2\text{O}(\text{g})$  reaction and the CRC for  $\text{ZrO}_2(\text{s}) / \text{D}_2\text{O}(\text{g})$ . The values and those reported by Barin and Cordfunke are indistinguishable for temperatures below 2200K. For temperatures above 2200K, Barin reports fairly constant values whereas Cordfunke reports decreasing values for the heat of reaction. This may be because constant Cp values are reported by Barin above 1478K whereas increasing Cp values above 1478K and increasing non-linearity in Cp values with increasing temperature above 2000K are reported by Cordfunke. This indicates that the Cp values reported by Cordfunke are more appropriate for high temperatures. Therefore, for temperatures above 2200K, the values quoted from Cordfunke are recommended.

To assess if there is any significant differences if the reaction  $\text{ZrO}_2(\text{s}) / \text{D}_2\text{O}(\text{g})$  was considered, Barber<sup>4</sup> reported, using the CRC data, that the difference in the heat of formation of heavy water compared to light water is about 3% at 300K decreasing to about 1.7% at 1500 K. Also, he reported that the heat of reaction for the zirconium-steam reaction calculated for heavy water is slightly lower (see Figure 1) magnitude than the values based on Cordfunke data.

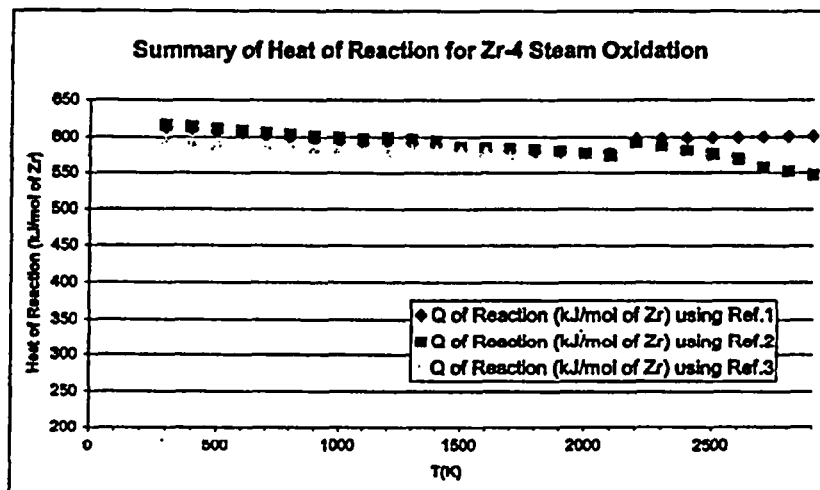


Figure 1: Heat of reaction for Zr-4 steam oxidation from various sources.

## 2.2 Melting Temperature

Several authors have measured the melting temperature of Zircaloy-4. The melting temperature value of pure zirconium is 2123 K. Zircaloy-4 has a value lower than this because the melting temperature, of the Zircaloy alloys used for fuel sheath, has various contents of tin and oxygen. For CANDU sheaths, Rossinger<sup>5</sup> reported a value of  $2033 \pm 10$  K. Recently, Hayward and George<sup>6</sup> obtained values of 2034 K, 2034 K, 2037 K and 2036 K, using differential thermal analysis technique, with an estimated uncertainty of 20 K. Based on this recent results, we recommend a melting temperature value for CANDU Zircaloy-4 of  $2035 \pm 20$  K.

### 3 FROM 3 Validation

#### 3.1 Phenomenon Modeled

The phenomenon modelled by FROM 3 is identified in The Fuel and Fuel Channel Validation Matrix<sup>7</sup> as FC9 - Sheath Oxidation or Hydriding. In particular, FROM 3 simulated only the Zircaloy-4 oxidation in steam. The tests selected are identified in the Validation Matrix as: SE13 and SE47.

#### 3.2 Experimental data selection

After a extensive literature search and elimination of duplicated cases, a data base containing 163 isothermal tests corresponding to 13 different isothermal and 70 temperature transient cases, was compiled. Figure 2 schematically shows the three types of temperature transients used in the transient experiments. The heating rates (HR) ranged from 45 to 128 K/s; cooling rates (CR) from 2.2 K/s to quench; maximum temperatures ranged from 1173 to 1873 K and tests were performed with various holding times (HT). The source of these data are 163 isothermal and 6 transient cases performed by Cathcart et al.<sup>8</sup>, 21 transients by Leistikow et al.<sup>9</sup> and 43 by Sagat et al.<sup>10</sup>.

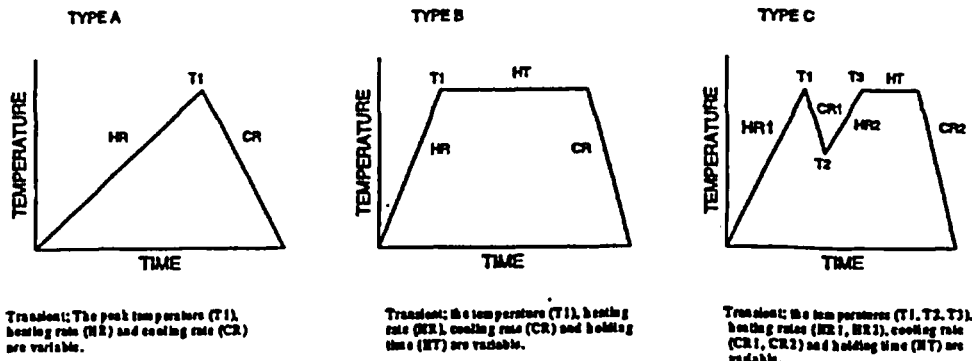


Figure 2: Graphical representation of the form of temperature transients used throughout test cases.

#### 3.3 Results

The sample geometries, oxidizing conditions, sample temperatures in function of time and oxide and alpha layer thicknesses were obtained from the above references. This information was used in the preparation of FORM 3 input files and the simulation performed. The code predictions and measured values are presented in Table 1.

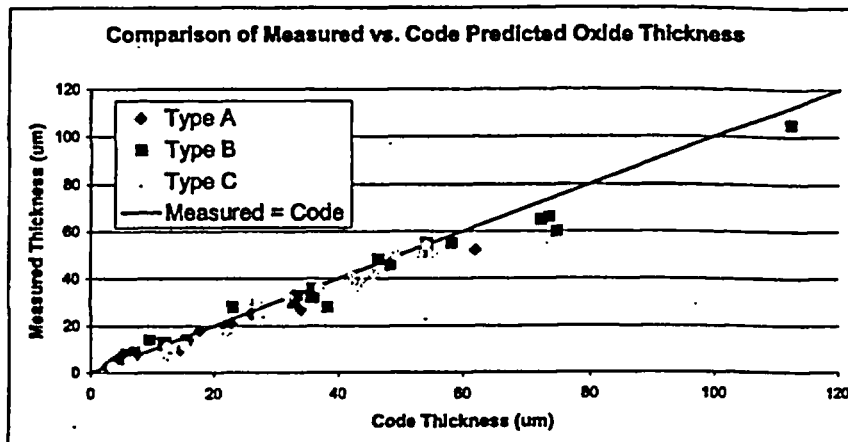


Figure 3: Experimental values and FROM 3 predictions

To assessment of these results, performed using a statistical approach was done to gain a more quantitative understanding of FROM simulation biases.

### 3.4 Validation Assessment

Validation of the FROM 3 code requires that the user be confident that it is capable of predicting the alpha and oxide layer growth during a high temperature transient, such as a LOCA. This paper follows the approach derived in Reference 11. The database of 13 isothermal and 70 transient experiments, including those that focus basic assumptions and abilities of FROM 3 and those indicative of postulated accident conditions, are used to compare against code results. For validation purposes, the solutions for 'true' oxide thickness,  $y$ , are assumed to be of simple mathematical form, i.e.:

$$y = f(y_c) + \varepsilon_c \quad (1)$$

where  $y_c$  is the code thickness prediction and  $\varepsilon_c$  the unknown random error in code computation. The parameters of this function are estimated based on different types of divergence between the code's predictions and the true thicknesses. Confidence intervals for the true parameter values are determined and finally, the parameter estimates are used to produce an estimate of the true thickness and an overall confidence interval.

Measurement of both alpha and oxide thickness is assumed to be susceptible to a *random error* and a combination of *offset* and *multiplicative bias*. The measurement bias is quantified with a linear back-projection in time technique (to  $T=0$ ). This basis for a single case confidence interval, which, provides an overall confidence interval and a statistical test for the null hypothesis; whether the code approximation is adequate (within an acceptable confidence interval) or not adequate (it falls outside the range or applicable thickness values and therefore an adjustment provided by  $f$  is necessary).

The measured and true thickness values are assumed to be related in the following form:

$$y_M = \mu_M + b_M y + \varepsilon_M \quad (2)$$

where  $\mu_M$  is the additive component or bias,  $b_M$  is the multiplicative component, and  $\varepsilon_M$  is a random error, independent of the true thickness  $y$ .

It can also be shown that  $f(y_c)$  is a linear function of  $y_c$  with the use of a General Additive Model applied to the three types of experimental cases available (see reference 1). Correlation coefficients for such a process are typically between 0.96 and 0.99 and hence a strong indication for linearity.

Therefore, we can say:

$$y_c = \mu_c + b_c y + \varepsilon_c \quad (3)$$

where  $\mu_c$  is the code bias, and  $b_c$  is the code multiplicative component.

By regressing  $y_M$  against  $y_c$ , assuming that the multiplicative error in measurement (alpha or oxide layer),  $b_M \approx 1$ , and assuming that a separate estimate for  $\mu_M$  is available, estimates of the code errors can be obtained with:

$$\mu_c = \mu_R - \mu_M \quad (4)$$

and:

$$b_c = b_R \quad (5)$$

where  $\mu_R$  is the intercept parameter in the general regression model (of  $y_M$  against  $y_c$ ) and  $b_R$  is the slope parameter in the same.

In time, we can write:

$$y_M(t) = \mu_M + b_M y(t) + \varepsilon_M, \quad t \geq t_s \quad (6)$$

for constant  $\mu_M$  and  $b_M$ . A hypothetical projection to 'time zero' for an arbitrary set of data will give:

$$\mu_M = y_M(0) - \varepsilon_M - b_M y(0) \quad (7)$$

We know that  $y_D(0) = 0$ , and assume that  $y_a(0) = 0$ . Therefore, we reduce the previous to an estimation of the measurement bias by backward projection:

$$\mu_M = E[y_M(0)] \quad (8)$$

where  $E[y_M(0)]$  is the expected value of  $y_M(0)$ .

For the code results, we have the similar:

$$y_M(t) = \mu_R + b_R y_C(t) + \varepsilon_R(t) \quad (9)$$

which for a starting thickness of  $y_C(0)$ , the bias in code prediction becomes:

$$\mu_C = -b_R y_C(0) \quad (10)$$

This process is only good for Type A and isothermal cases where predicted and/or measured thicknesses can be projected back in time to the beginning of the heating period. For those cases which backward projection is not applicable, we use an estimation by averaging; that is, by assume the measurement bias is the average of the previous biases or:

$$\mu_M = \overline{\mu_M} = \frac{1}{k} \sum_{j=1}^k \mu_{Mj} \quad (11)$$

where  $k$  is number of previous estimates. Hence:

$$\mu_C = \mu_R - \overline{\mu_M} \quad (12)$$

Determination of the confidence interval is carried out by assuming that the errors in the regression of  $y_M$  against  $y_C$  follow a Normal distribution:

$$\varepsilon_R \sim N(0, \sigma_R^2) \quad (13)$$

where an estimate of the variance,  $\sigma_R^2$ , is given by:

$$s_R^2 = \sum_{i=1}^n (y_{Mi} - \hat{y}_{Mi})^2 / (n-2) \quad (14)$$

where the summation is known as the SSR or Residual Sum of Squares.

With an expression for the confidence interval, we can move ahead to derive estimates for measurement bias, code multiplicative error, code bias, and prediction of true thickness. Additionally, each can be done as before, through both backward projection and bias averaging.

Measurement bias by backward projection using (8) and variance of the estimator is as:

$$\sigma_{\hat{\mu}_M}^2 = \sigma_R^2 \left[ \frac{1}{n} + \frac{(y_C(0) - \bar{y})^2}{\sum_{i=1}^n (y_{Ci} - \bar{y}_C)^2} \right] \quad (15)$$

Given a normal distribution, the limits of  $(1 - \alpha)$ , the Confidence Interval for  $\mu_M$  is as follows:

$$\hat{\mu}_M \pm \hat{\sigma}_{\hat{\mu}_M} t_{n-2, 1-\alpha/2} \quad (16)$$

Using a finite  $s_R^2$  in place of an infinite  $\sigma_R^2$ , and  $t_{n-2, 1-\alpha/2}$  is the  $(1 - \alpha/2)$  percentile of the t-distribution with  $(n-2)$  degrees of freedom. For a 95 percent CI,  $\alpha = 0.05$ .

The process for a measurement bias estimate obtained by averaging is done by the same process, but redefining the variance as:

$$\sigma_{\hat{\mu}_M}^2 = \frac{1}{k^2} \sum_{j=1}^k \sigma_{\hat{\mu}_{Mj}}^2 \quad (17)$$

and the  $(1 - \alpha)$  CI of  $\bar{\mu}_M$  are given by:

$$\hat{\mu}_M \pm \sigma_{\hat{\mu}_M} z_{1-\alpha/2} \quad (18)$$

where  $z_{1-\alpha/2}$  is, for this time, the  $(1-\alpha/2)$  percentile of the standard normal distribution.

Code multiplicative error is, in all cases, the regression estimate of the slope of  $y_M$  against  $y_C$ . Hence, the variance is given by  $\sigma_R^2$  divided by the SSR, and the CI is based upon the t-distribution (see (15) and (16)).

$$\hat{b}_R \pm \frac{s_R}{\sqrt{\sum_{i=1}^n (y_{Ci} - \bar{y}_C)^2}} t_{n-2, 1-\alpha/2} \quad (19)$$

where  $s_R$  is the square of the variance of  $\epsilon_R$ .

A code bias estimate obtained by backward projection is calculated with:

$$\hat{\mu}_C = -\hat{b}_R y_C(0) \quad (20)$$

with variance of:

$$\sigma_{\hat{\mu}_C}^2 = y_C(0)^2 \sigma_{\hat{b}_R}^2 \quad (21)$$

and CI limits for  $\mu_C$  defined by:

$$-\hat{b}_R y_C(0) \pm s_{\hat{b}_R} |y_C(0)| t_{n-2, 1-\alpha/2} \quad (22)$$

The total variance to required to find the code bias estimate obtained by averaging,  $\sigma_{\hat{\mu}_C}^2$ , is found as the sum of two independent components; that in the estimate of the regression intercept parameter,  $\sigma_{\hat{\mu}_R}^2$ , and that in the estimate of the measurement bias,  $\sigma_{\hat{\mu}_M}^2$ . The limits on the CI for  $\hat{\mu}_C$  are approximated as:

$$\hat{\mu}_C \pm \sqrt{s_{\hat{\mu}_R}^2 + \hat{\sigma}_{\hat{\mu}_M}^2} z_{1-\alpha/2} \quad (23)$$

where  $s_{\hat{\mu}_R}^2$  is the regression estimate of the variance of  $\hat{\mu}_R$ :

$$s_{\hat{\mu}_R}^2 = s_R^2 \left[ \frac{1}{n} + \frac{\bar{y}_C^2}{\sum_{i=1}^n (y_{Ci} - \bar{y}_C)^2} \right] \quad (24)$$

For the prediction of true thickness, the estimation is initially given as:

$$\hat{y} = \hat{\mu}_C + \hat{b}_R y_C = \hat{\mu}_C + \hat{b}_R y_C \quad (25)$$

for an estimate obtained by backward projection for the true thickness prediction,  $\hat{y}$  has variance:

$$\sigma_{\hat{y}}^2 = (y_C - y_C(0))^2 \sigma_{\hat{b}_R}^2 \quad (26)$$

and limits of the CI for  $y$  are given by:

$$\hat{y} \pm |y_C - y_C(0)| s_{\hat{b}_R} t_{n-2, 1-\alpha/2} \quad (27)$$

Estimates for true thickness prediction obtained by averaging are, similar to the average of the code bias, based on the summation of variance:

$$\sigma_{\hat{y}}^2 = \sigma_{\hat{y}_M(y_C)}^2 + \sigma_{\hat{\mu}_M}^2 \quad (28)$$

where the variance of the prediction  $\hat{y}_M(y_C)$  is given by:

$$\sigma_{\hat{y}_M(y_c)}^2 = \sigma_R^2 \left[ \frac{1}{n} + \frac{(y_c - \bar{y}_c)^2}{\sum_{i=1}^n (y_{ci} - \bar{y}_c)^2} \right] \quad (29)$$

As before, the limits of the CI for  $y$  are defined by:

$$\hat{y} \pm \sqrt{\hat{\sigma}_{\hat{y}_M(y_c)}^2 + \hat{\sigma}_{\hat{\mu}_M}^2} z_{1-\alpha/2} \quad (30)$$

where  $\hat{\sigma}_{\hat{y}_M(y_c)}^2$  is obtained using  $s_R^2$  in place of  $\sigma_R^2$ .

Regression estimates for  $\mu_R$  and  $b_R$  are calculated for each test case with enough data points. Since computational errors are small compared to measurement errors, the random measurement error variance,  $\sigma_M^2$ , is approximated by the sample variance of  $\epsilon_R$ ,  $s_R^2$ . The isothermal cases are used to calculate the estimate of the measurement error variance. This value is found to be 3.3% of the alpha measurement and 2.6% of the oxide measurement.

The assumption that  $\epsilon_R$  is Normally distributed can be shown to be sound with the use of the Kolmogorov-Smirnov Test for goodness of fit.

Oxide measurement bias is estimated using backward projection for all isothermal and Type A cases, and the use of the average of those values for the Type B and C cases. This value,  $\hat{\mu}_{Mo}$ , is found to be  $3.1 \mu m$ . It's associated variance is  $0.094 \mu m^2$ .

In the same way, the alpha measurement bias,  $\hat{\mu}_{M\alpha}$ , is found to be 4.07. It's associated variance is  $0.394 \mu m^2$ .

Figure 1 shows the relation between the measured thickness and the limits of the 95% confidence intervals for the true oxide thickness for an isothermal case at 1677 K. Similar data for all Type C cases is shown in Figure 2. Note that the code generally over predicts the oxide growth thickness value.

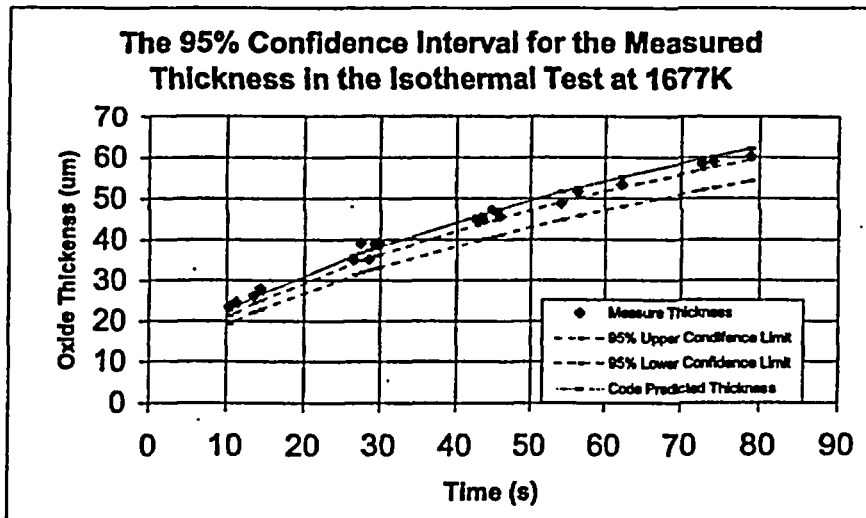


Figure 4: Measured and computed transient oxide thicknesses for isothermal test at 1677K.

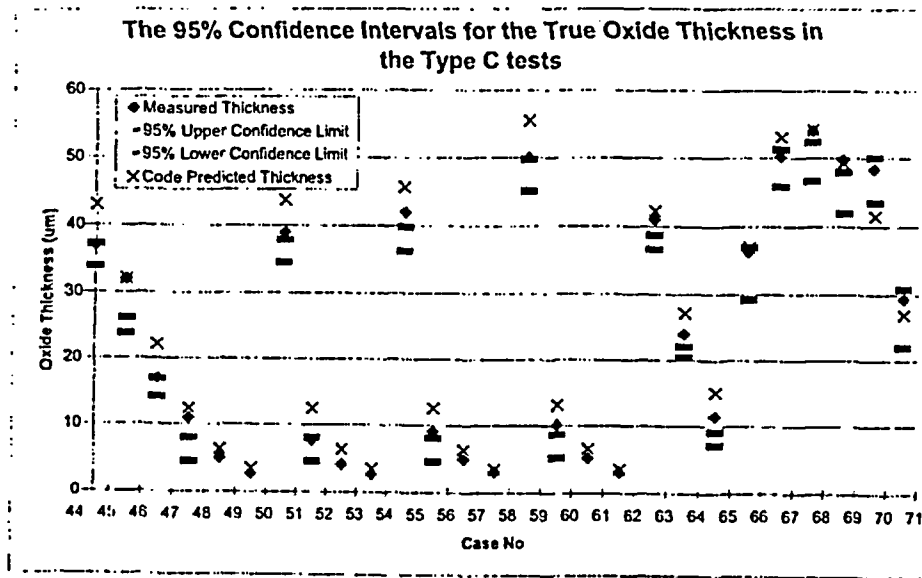


Figure 5: Final measured and computed oxide thicknesses for all Type C cases.

A final summary of all data analysis is shown directly in Table 1. Note that in all cases, the multiplicative parameter  $b_M = 1$ . With these results at hand, we can conclude that FROM 3 is a validated computer code for the type of application use described. Hence, FROM 3 has been incorporated into simulation codes (eg. FACTAR) for performing safety and licensing analysis.

## Code Prediction Relative to 95% Confidence Limits for True Thickness

Isothermal			Type A			Type B			Type C		
Temp	Alpha	Oxide	Case	Alpha	Oxide	Case	Alpha	Oxide	Case	Alpha	Oxide
1178	—	*	1.	*	H	16	H	H	44	*	H
1229	—	H	2	H	*	17	H	H	45	*	H
1274	H	L	3	—	—	18	H	H	46	*	H
1323	H	*	4	H	*	19	H	H	47	*	H
1374	*	*	5	H	*	20	H	H	48	—	—
1426	H	H	6	—	—	21	H	H	49	—	—
1476	H	H	7	—	H	22	H	H	50	*	H
1526	H	H	8	—	H	23	H	H	51	*	H
1577	*	H	9	H	H	24	H	H	52	—	—
1625	*	*	10	H	H	25	H	H	53	—	—
1677	H	H	11	H	H	26	*	H	54	*	H
1727	H	H	12	—	—	27	H	H	55	*	H
1777	H	*	13	*	H	28	—	*	56	—	—
			14	*	H	29	—	H	57	—	—
			15	H	*	30	H	H	58	*	H
						31	H	H	59	*	H
						32	H	H	60	—	—
						33	H	H	61	—	—
						34	H	H	62	L	H
						35	H	H	63	*	H
						36	H	H	64	H	H
						37	H	H	65	—	H
						38	H	H	66	—	H
						39	—	*	67	—	H
						40	—	*	68	—	H
						41	—	*	69	—	H
						42	H	H	70	—	*
						43	H	H			

Table 1: Code Prediction Relative to 95% Confidence Limits for True Thickness  
 H—Above Upper Limit; L—Below Lower Limit; \*—Within Limits

### 4 Comparison between FROM 3 and FROM.SFD

FROM.SFD was developed from FROM2 to add the capability to model Zircaloy/ $UO_2$  interaction (ie. The reduction of  $UO_2$  in contact with the sheath as time at high temperatures progresses) through up to seven oxide layers (or phases) with distinct material properties. Steam starvation (via a gap) and breakaway oxidation at low temperatures are also implemented. To compare, FROM 3 models resultant oxide growth from three oxide layers at temperature  $T > 1520^\circ C$ .

With validation complete for FROM 3, we can perform a comparison between the results of oxide layer growth from FROM.SFD against FROM 3 to gain similar confidence in the results from FROM.SFD. Note that with the gap between the fuel and the sheath modelled open in FROM.SFD, and the number of regions specified as 2, FROM.SFD results reduce to that equivalent of FROM 3.

#### 4.1 Case selection

10 cases from the experimental database of 163 isothermal cases and 70 transient cases are selected to compare predictions for oxide growth from the two codes. These cases are chosen to be representative of the codes capabilities under fast heating and cooling conditions as well as a large LOCA transient postulated to occur in a CANDU reactor for direct application to safety analysis.

#### 4.2 Results

Predictions for ZrO<sub>2</sub> layer thickness from both codes has been found to be excellent. Differences between FROM.SFD and FROM 3 are below 1% for 8/11 cases and within 5% for the remaining. Note that the experimental error associated with all measured values is approximately 14%. These results indicate that FROM.SFD predicts oxide layer thickness very close to FROM 3 predictions as well as to measured values.

<b>Comparison Between FROM 3 and FROM.SFD Predictions</b>						
<b>Case</b>	<b>FROM 3 Results (um)</b>		<b>FROM.SFD Results</b>		<b>% Diff</b>	
	<b>ZrO<sub>2</sub></b>	<b>alpha</b>	<b>ZrO<sub>2</sub></b>	<b>alpha</b>	<b>ZrO<sub>2</sub></b>	<b>alpha</b>
3	21.28	18.11	21.1	20.9	0.85%	15.41%
5	34.04	39.92	33.9	40.7	0.41%	1.95%
12	17.64	15.88	17.6	23.6	0.23%	48.61%
19	53.93	74.25	53.5	73.5	0.80%	1.01%
20	33.09	36.73	32.7	37.4	1.18%	1.82%
26	119.7	143.3	114.1	153.4	4.68%	7.05%
43	33.21	36.83	32.9	41.9	0.93%	13.77%
54	45.66	52.94	45.4	62	0.57%	17.11%
65	37.04	40.28	36.8	43.5	0.65%	7.99%
66	53.1	69.26	52.5	76.5	1.13%	10.45%
LOCA	8.34	9	9	9.4	7.91%	4.44%

Table 2: Comparison of FROM code results.

## 5 Summary

In this paper, recommended values for the heat of reaction and melting temperature for the CANDU sheath material, Zircaloy-4, are presented. Also, comparison of FROM 3 code prediction with experiments has been performed and a statistical assessment of the code biases has been obtained. Finally, a comparison between FROM 3 and FROM.SFD in their common region of applicability was also performed.

## 6 References

- 1 Barin, I., "Thermochemical Data for Pure Substances", 3<sup>rd</sup> edition, Weinheim, New York, 1995.
- 2 E.H.P. Cordfunke (Editor), "Thermochemical Data for Reactor Materials and Fission Products", North Holland Publishing Company, Amsterdam, 1990.
- 3 R.C. Weast (Editor), "CRC Handbook of Chemistry and Physics", 60th Edition CRC Press, Boca Raton, Florida, 1980.
- 4 D.H. Barber, "Heat of Zircaloy-Steam Reaction in Heavy Water" File N-06631.01 P, 1997.
- 5 H.E. Rosinger, "Melting Temperature of Zircaloy-4", AECL SAB-83-53, 1983.
- 6 P.J. Hayward and J.M. Gerge, "Determination of the Solidus Temperature of Zircaloy-4/Oxygen Alloys", Journal of Nuclear Materials 272(1999)294.
- 7 "A Phenomenology-Based Matrix of Tests for Use in Validation of Fuel and Fuel Channel Thermal-Mechanical Behaviour Codes Employed in CANDU Safety Analysis". Revision 1, N-08131.02-P- Ontario Hydro, 1998.
- 8 J.V. Cathcart, R.E. Powel, R.A. McKee, R.E. Druschel, G.J. Yurek, J.J. Campbell and S.H. Jury, "Zirconium Metal-Water Oxidation Kinetics IV. Reaction Studies" ORNL/NUREG-12 and 17 (1977).
- 9 S. Leistikov, G. Schanz and H.V. Berg, "Investigation into the Temperature Transient Steam Oxidation of Zircaloy-4 Cladding Material Under Hypothetical PWR Loss-of-Coolant Conditions, KFK 2810 (1979).
- 10 S. Sagat, T.J. Hoffman and D.E. Foote, "Transient Oxidation of Zircaloy-4 Fuel Sheaths in Steam" AECL Report CRNL-2521, 1983.
- 11 L. Chee, "Validation of FROM3 - Full Range Oxidation Model for Zircaloy-4, Ver 3", Report No. 6268-030-1997-RA-001-R00, Ontario Hydro Technologies, 1998.